Eur. Phys. J. B **47**, 251–254 (2005)
DOI: 10.1140/epjb/e2005-00315-0

THE EUROPEAN PHYSICAL JOURNAL B

# The instability of chaotic synchronization in coupled Lorenz systems: from the Hopf to the Co-dimension two bifurcation

J. Yang[1,a] and M. Zhang[2]

[1] School of Science, Beijing University of Posts and Telecomunications, Beijing, 100876, P.R. China
[2] Center for Advanced Study, Tsinghua University, Beijing, 100084, P.R. China

Received 19 January 2005 / Received in final form 12 July 2005
Published online 11 October 2005 – 

**Abstract.** We investigate the Hopf bifurcation of the synchronous chaos in coupled Lorenz oscillators. We find that the system undergoes a phase transition along the Hopf instability of the synchronous chaos. The phase transition makes the traveling wave component with the phase difference $\phi(i) - \phi(i+1) = 2\pi/N$ between adjacent sites unstable. The phase transition also plays a role to relate the Hopf bifurcation with the co-dimension two bifurcation of the synchronous chaos.

**PACS.** 05.45.Xt Synchronization; coupled oscillators – 05.45.-a Nonlinear dynamics and nonlinear dynamical systems

## 1 Introduction

In recent years, synchronization in coupled chaotic oscillators has been studied extensively due to its theoretical interests and practical applications [1]. As an invariant attractor, the instabilities of the synchronous chaos have drawn lots of attentions. Generally, there are three types of bifurcations associated with the synchronous chaos. The first type is the short wave bifurcation (SWB) [2] in the sense that its unstable spatial mode has the shortest wavelength. SWB occurs when the diffusion coupling increases beyond a critical value. It can be observed only in a certain type of systems [3]. The second one is the Hopf bifurcation that develops in asymmetrically coupled oscillators when the gradient coupling becomes sufficiently large, causing a pair of complex conjugate spatial modes unstable. As a result, a traveling wave component (TWC) appears with the synchronous chaos being its background. The Hopf bifurcation of the synchronous chaos was first found in coupled Lorenz oscillators [3,4]. Lately this kind of bifurcation was seen in other systems such as coupled Duffing oscillators [5], coupled Rossler systems, and the coupled map lattice [6]. The third type is the co-dimension two bifurcation that is evoked by decreasing the diffusion coupling in symmetrically coupled systems where two same eigenmodes become unstable simultaneously. Immediately after the synchronous chaos breaks down, the partial synchronization (PAS) can be observed [7]. For example, the realized PAS for $N = 4$ is "aabc" where different alphabet represents different dynamical state.

[a] e-mail: jzyang@bupt.edu.cn

Related to the Hopf and the co-dimension two bifurcation of the synchronous chaos, several problems are to be addressed. First, according to the theory in references [3,4], the Hopf bifurcation should exist in any coupled chaotic oscillators (maps) so long as the oscillators (maps) are coupled in an asymmetrical way. Unfortunately, the indicator of the Hopf bifurcation – the traveling wave superimposed on chaotic background – cannot display in many systems. Secondly, though there are many possible states of PAS immediately after the co-dimension two bifurcation goes away, the number of realized is limited. As an example, the state of PAS for $N = 6$ is either "adabcb" or "abbacc" even though there are totally six possible PAS states right after the synchronous chaos becomes unstable [7]. Can we find a reasonable explanation without calculating the transversal Lyapunov exponents? Last, the Hopf and the co-dimensional two bifurcation meet when the critical gradient coupling becomes zero. It is intriguing to explore how the crossover from one bifurcation to the other happens. These are our motivations to conduct the study in this letter.

## 2 The Hopf instability of synchronous chaos

The system under investigation is coupled Lorenz oscillators:

$$\begin{cases} \dot{x}(j) = \sigma(y(j) - x(j)) \\ \dot{y}(j) = \rho x(j) - y(j) - x(j)z(j) + (\epsilon + r)(x(j+1) - x(j)) \\ \qquad\quad + (\epsilon - r)(x(j-1) - x(j)) \\ \dot{z}(j) = x(j)y(j) - \beta z(j) \end{cases} \qquad (j = 1, \ldots, N),$$

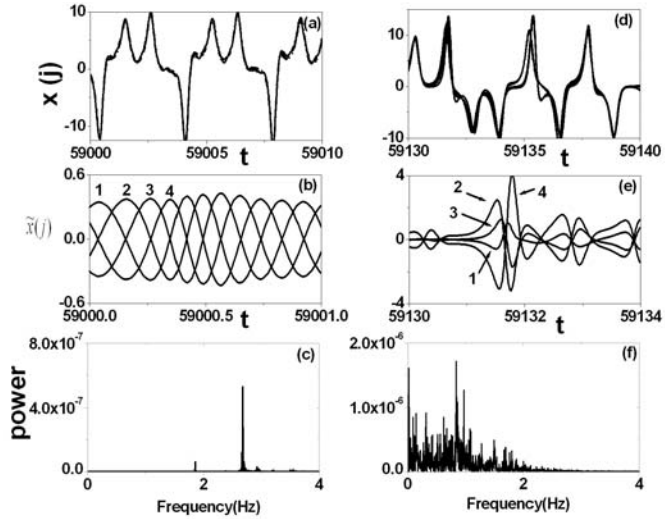


**Fig. 1.** $\epsilon = 14$, $r = 7.95$, and $N = 4$ in (a)–(c). (a) the time evolution of $x(j)$, $j = 1, \ldots, 4$. Roughly, the trajectories of the four sites are the same; (b) the time evolution of $\tilde{x}(j)$, $j = 1, \ldots, 4$. The wave pattern is exhibited; (c) the power spectrum of $\tilde{x}(j)$, which shows at around 2.6 a sharp peak. $\epsilon = 2.5$, $r = 1.2$, and $N = 4$ in (d)–(f), where the time evolution of $x(j)$, $\tilde{x}(j)$, and the power spectrum of $\tilde{x}(j)$ are shown in the same order as in (a)–(c). The background chaos is still almost the same for four sites, but the wave pattern does not show up in $\tilde{x}(j)$, instead it has a broadband power spectrum.

where the periodic boundary condition $\boldsymbol{u}(j) = \boldsymbol{u}(j+N)$ is applied on $\boldsymbol{u}(j) = (x(j), y(j), z(j))$. The parameters $\epsilon$ and $r$ represent the diffusion and gradient couplings, respectively. We take $\sigma = 10$, $\rho = 28$, and $\beta = 1$, under which condition the single Lorenz oscillator is in a chaotic state. With sufficiently large $\epsilon$ the synchronous chaos $\boldsymbol{u}(j,t) = \boldsymbol{s}(t)$ is stable for small $r$, where $\boldsymbol{s}(t)$ is the chaotic orbit of the single Lorenz system. As $r$ increases over a critical value $r_c$, a pair of complex conjugate spatial modes become unstable and the synchronization breaks down. Figures 1a–1c show such a case for $N = 4$. At first glance, the trajectories of the four sites are the same, while a scrutiny on their fine structures does reveal some tiny differences. To single out the discrepancies, we calculate the quantity $\tilde{x}(j) = x(j) - \sum_{j=1}^{4} x(j)/4$ for each site $j$. The traveling wave pattern with the phase difference $\Delta\phi = 2\pi/N$ between the adjacent sites is found in Figure 1b. The power spectrum of $\tilde{x}(1)$ shows a sharp peak located at the generalized rotation number of the unstable modes. The results in Figures 1a–1c show clearly the Hopf bifurcation of the synchronous chaos. According to the knowledge of the Hopf bifurcation for the fixed point and periodic solution, we expect to find the indicator of the Hopf bifurcation of the synchronous chaos, TWC superimposed on the background chaos (we use this term in the rest of the letter when the synchronous chaos is unstable), for arbitrary $\epsilon$'s. But the finding is quite counter to our intuition when we decrease $\epsilon$. In Figures 1d–1f, we show the results for $\epsilon = 2.5$ ($r_c \approx 1.2$). Though the background chaos is still almost the same for each site, the wave structure of $\tilde{x}(j)$ disappears. Instead, the power spectrum of $\tilde{x}(1)$ becomes chaotic broadband. Comparing Figures 1d–1f with Figures 1a–1c, we find in Figures 1d–1f that the instantaneous period of $\tilde{x}(j)$ fluctuates vehemently and the phase differences between the successive sites, $\Delta\phi$'s, deviate from $2\pi/N$.

## 3 The phase transition connecting the Hopf and the co-dimension two bifurcations of synchronous chaos

Considering the facts that the background chaos is not exactly synchronous and the on-off intermittence occurs from time to time [8], the background chaos should have some noiselike effect on TWC that manifests itself by fluctuations of the amplitude and the period of TWC. To learn how the background chaos influences the dynamics of TWC, it is helpful to work on the phase of $\tilde{x}(j)$. Before we go on, we need to give a working definition of the phase. The one utilizing $\tilde{x}(j)$ and $\tilde{y}(j)$ previously employed in many literatures [7,9] does not work well in this problem. We show in Figure 2a $\phi(2)$ versus $\phi(1)$ under this definition with the same parameters as in Figure 1a. Theoretically, we know $|\phi(2) - \phi(1)| = \pi/2$ (or $3\pi/2$) since TWC has a wavelength $L = 4$. Nevertheless the results in Figure 2a do not comply with the relation. Another definition of phase using $\tilde{x}(j,t)$ and $\tilde{x}(j,t+\tau)$ is widely adopted to determine the phase singularity in the spatio-temporal system [10]. The phase is defined as $\phi(j) = \arctan[\tilde{x}(j,t+t')]/\tilde{x}(j)$ where $t'$ is the time delay. $\phi(2)$ versus $\phi(1)$ is shown in Figure 2b and they obey the relation $|\phi(2) - \phi(1)| = \pi/2$ quite well except for small fluctuations. Actually, a proper choice of $t'$ is necessary for the measurement of the phase, otherwise the phase distorts a lot. Some simple algebraic calculations show that the best choice of $t'$ is $T/4$, where $T$ is the period of $\tilde{x}(j,t)$. Since $\tilde{x}(j,t)$ is modulated by the background chaos and its period fluctuates in a certain range, $t'$ cannot be determined uniquely. To lower the uncertainty, we take the average of the phases for several $T$ around the period that corresponds to the largest peak in the power spectrum. A typical trajectory of the phase difference $\Delta\phi_{i,j} = \phi(j) - \phi(i)$ for $i = 1$ and $j = 2$ is plotted in Figure 2c. It fluctuates around $3\pi/2$ and has the same period as $\tilde{x}(j,t)$. Correspondingly, $\Delta\phi_{1,3}$ fluctuates around $\pi$ and its amplitude is much smaller than that of $\Delta\phi_{1,2}$ (the results are not shown here). The power spectrum of $\Delta\phi_{1,2}$ is shown in Figure 2d. The peak locates at the frequency with which $\tilde{x}(j,t)$ oscillates. There is an unexpected finding in Figure 2d where we use the log-log scale. The low frequency part follows a power law $P(f) = f^{\gamma}$ with the exponent $\gamma = -2$. The same power law exists for the low frequency part in the power spectrum of $\Delta\phi_{1,3}$ which does not have the apparent peak presented in that of $\Delta\phi_{1,2}$. The power law here indicates that the background chaos drives the phase difference to fluctuate in a fashion of random walk just as the white noise does [11]. It is quite interesting because the background chaos has an intrinsic structure in

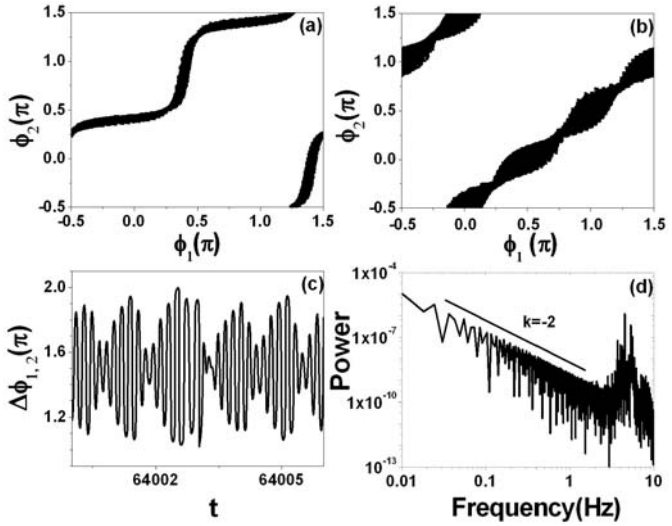


**Fig. 2.** $\epsilon = 14$, $r = 7.95$. (a) $\phi(2)$ versus $\phi(1)$ by using $\tilde{x}(j)$ and $\tilde{y}(j)$ to define the phase of the site $j$. We have rescaled $\phi(j)$ by $\pi$; (b) $\phi(2)$ versus $\phi(1)$ by using $\tilde{x}(j,t)$ and $\tilde{x}(j,t+\tau)$ to define the phase of the site $j$; (c) a typical trajectory of $\Delta\phi_{1,2}$; (d) the power spectrum of $\Delta\phi_{1,2}$, which shows both a power law in the low frequency and a large peak at the same frequency as in Fig. 1c. The line in this plot has a slope of $-2$.

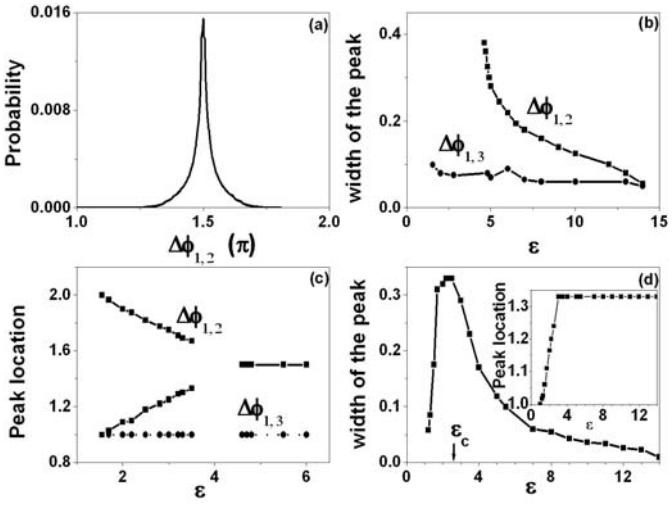


**Fig. 3.** $N = 4$ in (a)–(c). (a) the distribution of $\Delta\phi_{1,2}$, which has a sharp peak at $3\pi/2$. Parameters are the same as in Figure 2; (b) the peak widths of $\Delta\phi_{1,2}$ and $\Delta\phi_{1,3}$. We have amplified $\Delta\phi_{1,3}$ 1000 times; (c) the peak locations of $\Delta\phi_{1,2}$ and of $\Delta\phi_{1,3}$. The former shows a phase transition while the latter freezes at $\pi$; (d) the peak width versus $\epsilon$ for $N = 3$. the inset shows the peak location versus $\epsilon$. A phase transition is also seen in this plot.

the power spectrum while the white noise has no such a structure.

To further investigate the effect of the background chaos on TWC, we consider how the distribution of $\Delta\phi_{i,j}$ changes with the coupling constant $\epsilon$ along the onset of the instability of the synchronous chaos. An example of the distribution of $\Delta\phi_{1,2}$ is presented in Figure 3a. The center of the peak locates at $3\pi/2$ in this plot. Usually, for a stochastic process, the location and the width of the peak are two quantities that describe the properties of the underlying process. The peak width characterizes the fluctuation strength while the peak location plays an important role when there exists a certain phase transition. To stress the impact of the background chaos on TWC, we first explore the peak width that is defined as the range when the probability is half the peak value. Figure 3b shows the peak width versus the diffusive coupling $\epsilon$. For large $\epsilon$ the peak width is small, which in turn tells that the impact of the background chaos is weak. With the decrease of $\epsilon$ the width increases roughly in an exponential way in the parameter range we investigate, which means the smaller the diffusive coupling the stronger the fluctuation of the phase difference induced by the background chaos. The curve becomes much steeper when $\epsilon$ approaches 4.5. The plot also shows results for $\Delta\phi_{1,3}$. The width of $\Delta\phi_{1,3}$ is extremely narrower than that of $\Delta\phi_{1,2}$ and is almost a constant. A transition can be found in the figure of the peak location of $\Delta\phi_{1,2}$ [shown in Fig. 3c]. For large $\epsilon$, the peak locates at $3\pi/2$. However, the state with the peak location at $3\pi/2$ loses its stability for small $\epsilon$ and a state with a larger $\Delta\phi_{1,2}$ appears. The lower branch of the peak location is symmetric with respect to the upper one about $3\pi/2$. The upper (lower) branch stands for TWC where the second oscillator is lagging (leading) the first one. The existence of the two branches is attributed to the hopping of the system forced by the background chaos. Both the large slope in Figure 3b and the shift of the peak location indicate a phase transition due to the impact of the background chaos on TWC, i.e., a background-chaos-induced phase transition. Unexpectedly, we cannot determine whether or not the transition is continuous for $N = 4$ since we cannot investigate the parameter regime around $\epsilon = 4$ where an actual transition occurs. The underlain fact is that there exists a periodic traveling wave solution in this regime even when the synchronous chaos is still stable. Any small fluctuation will bring the system into the traveling wave solution once the synchronous chaos loses its stability. Such a parameter regime where the traveling wave is dominant grows with the increase of the system size. To evade this obstacle, we investigate the system with $N = 3$. The width of $\Delta\phi_{1,2}$ is shown in Figure 3d. For large $\epsilon$, the width increases with the decrease of $\epsilon$ in the same way as in the system with $N = 4$. After arriving at the maximum, the width decreases to zero with the decrease of $\epsilon$. The zero width is reached at $r_c = 0$ where the oscillators are symmetrically coupled with each other. The inset shows that the peak location changes with $\epsilon$. The transition takes place the time the maximum of the peak width is approached. Past the transition point, the peak location shifts from $4\pi/3$ to $\pi$ continuously. With the help of the results for $N = 3$, we extend to the case of $N = 4$ the conclusion that the phase transition is a continuous process.

Figure 3c also shows the peak location for $\Delta\phi_{1,3}$. Different from the one for $\Delta\phi_{1,2}$, there is no phase transition for $\Delta\phi_{1,3}$ implied by the shift of the peak location.

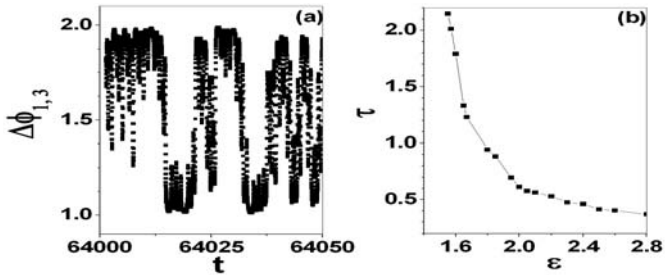


**Fig. 4.** (a) the time evolution of $\Delta\phi_{1,2}$, which jumps frequently between $\pi$ and $2\pi$. Here $\epsilon = 0.18, r = 0.365$; (b) $\tau$ versus $\epsilon$. The life time diverges when $r_c$ tends to zero.

Furthermore, in Figures 3b and 3d, the phase difference between adjacent sites becomes 0 or $\pi$ and the width also becomes zero when $\epsilon$ decreases till $r_c$ goes to zero. It suggests that the system forms two clusters in each of which the sites stay in phase even if their amplitudes are not synchronized. Actually the behaviors of $\Delta\phi_{1,3}$ ($\Delta\phi_{2,4}$) for $N = 4$ in Figures 3b and 3c tell us that $\Delta\phi_{1,3}$ is so stable that it has a strong resistance to the background chaos and that the relation $\Delta\phi_{1,3} = \pi$ holds regardless of the phase transition in $\Delta\phi_{1,2}$. The phase relation between sites 1 and 3 (sites 2 and 4) has two consequences: (1) It acts as a barrier that prevents site 2 (site 1) from falling into the same cluster as site 4 (site 3); (2) It is a rule responsible for the equal division of the system into two clusters. The rule can be readily extended to any even N where the phase difference of the sites $i$ and $i + N/2$ is $\pi$. For odd $N$, the system splits into two clusters which have adjacent $[N/2]$ and $[N/2]+1$ sites, respectively. We have confirmed it by performing the simulation for $N = 20$ and $N = 21$.

The phase transition along the Hopf instability of the synchronous chaos is the root that we cannot find the indicator of the Hopf bifurcation in many coupled systems. For example, in Figure 1d two clusters, within which the phase difference between adjacent sites is small, are already formed so the structure of TWC cannot show up.

Noticing that the two antiphase clusters form at $r_c = 0$, where the Hopf and the co-dimension two bifurcation meet, we find that PAS "adabcb" or "abbdcc" for $N = 6$ are eligible after the co-dimension two bifurcation. While other states such as "abcabc", "abbacc", "aabaab", and so on mentioned in [7], which cannot form two antiphase clusters, are only possible far away from the bifurcation point according to the discussion above. Besides, the continuous phase transition shown in Figure 3 proves that the crossover from the Hopf to the co-dimension two bifurcation of the synchronous chaos is a continuous process. The phase transition induced by the background chaos plays a critical role in this crossover, in other words, the phase transition is a must accompanying the continuous crossover between these bifurcations.

Finally we show how the system jumps between the two branches in Figure 3c for small $\epsilon$. Figure 4a shows a typical trajectory of $\Delta\phi_{1,2}$ which jumps back and forth between the upper and the lower branches stochastically when the state with $\Delta\phi_{1,2} = 3\pi/2$ is unstable. We define this unstable state as the boundary that separates the two branches, then we measure the average life time $\tau$ during which the system stays in one branch before it jumps to another one. $\tau$ is shown in Figure 4b and it roughly follows a power law with the exponent around 0.63. When $r_c = 0$, the average life time $\tau$ goes to infinity and the system stays in one branch forever.

## 4 Conclusion

In conclusion, we have investigated the Hopf bifurcation of the synchronous chaos in coupled Lorenz oscillators. We have found that the system undergoes a background-chaos-induced phase transition along the Hopf instability of the synchronous chaos. The phase transition makes TWC with $\Delta\phi_{1,2} = 2\pi/N$ between adjacent sites unstable. It is this phase transition that causes the disappearance of TWC. On the other hand, the phase transition induces the continuous crossover from the Hopf to the co-dimension two bifurcation which is characterized by the formation of the two antiphase clusters within which the phase difference is zero when $r_c = 0$.

This work was supported by the Grant No. 10405004 from Chinese Natural Science foundation.

## References

1. L.M. Pecora, T.L. Carroll, G.A. Johnson, D.J. Mar, J.F. Heagy, Chaos **7**, 520 (1997)
2. J.F. Heagy, T.L. Carroll, L.M. Pecora, Phys. Rev. Lett. **73**, 3528 (1994); J.F. Heagy, L.M. Pecora, T.L. Carroll, Phys. Rev. Lett. **74**, 4185 (1995)
3. G. Hu, J. Yang, W. Liu, Phys. Rev. E **58**, 4440 (1998)
4. G. Hu, J.Z. Yang, W.Q. Ma, J.H. Xiao, Phys. Rev. Lett. **81**, 5314 (1998)
5. W. Ma, J. Yang, W. Liu, et al., Acta Phys. Sin. - Ch. Ed. **48**, 787 (1999)
6. H.L. Yang, A.S. Pikovsky, Phys. Rev. E **60**, 5474 (1999)
7. G. Hu, Y. Zhang, H.A. Cerdeira, S. Chen, Phys. Rev. Lett. **85**, 3377 (2000); Y. Zhang, G. Hu, H.A. Cerdeira, S. Chen, T. Braun, Y. Yao, Phys. Rev. E **63**, 026211 (2001)
8. E. Ott, J.C. Sommerer, Phys. Lett. A **188**, 39 (1994)
9. M.G. Rosenblum, A.S. Pikovsky, J. Kurths, Phys. Rev. Lett. **78**, 4193 (1997)
10. R.A. Gray, A.M. Pertsov, J. Jolife, Nature **392** (1998)
11. H. Risken, *the Fokket-Planck Equation* (Springer-Verlag, 1984)